JOURNAL OF GEOPHYSICAL RESEARCH, VOL. 117, A00M06, doi:10.1029/2012JA017926, 2012

MESSENGER observations of a flux-transfer-event shower at Mercury

James A. Slavin,[1] Suzanne M. Imber,[1,2] Scott A. Boardsen,[3,4] Gina A. DiBraccio,[1] Torbjorn Sundberg,[3] Menelaos Sarantos,[3,4] Teresa Nieves-Chinchilla,[3,4] Adam Szabo,[3] Brian J. Anderson,[5] Haje Korth,[5] Thomas H. Zurbuchen,[1] Jim M. Raines,[1] Catherine L. Johnson,[6,7] Reka M. Winslow,[6] Rosemary M. Killen,[8] Ralph L. McNutt Jr.,[5] and Sean C. Solomon[9,10]

Received 11 May 2012; revised 6 September 2012; accepted 7 September 2012; published 30 October 2012.

[1] Analysis of MESSENGER magnetic field observations taken in the southern lobe of Mercury's magnetotail and the adjacent magnetosheath on 11 April 2011 indicates that a total of 163 flux transfer events (FTEs) occurred within a 25 min interval. Each FTE had a duration of ~2–3 s and was separated in time from the next by ~8–10 s. A range of values have been reported at Earth, with mean values near ~1–2 min and ~8 min, respectively. We term these intervals of quasiperiodic flux transfer events "FTE showers." The northward and sunward orientation of the interplanetary magnetic field during this shower strongly suggests that the FTEs observed during this event formed just tailward of Mercury's southern magnetic cusp. The point of origin for the shower was confirmed with the Cooling model of FTE motion. Modeling of the individual FTE-type flux ropes in the magnetosheath indicates that these flux ropes had elliptical cross sections, a mean semimajor axis of 0.15 R_M (where R_M is Mercury's radius, or 2440 km), and a mean axial magnetic flux of 1.25 MWb. The lobe magnetic field was relatively constant until the onset of the FTE shower, but thereafter the field magnitude decreased steadily until the spacecraft crossed the magnetopause. This decrease in magnetic field intensity is frequently observed during FTE showers. Such a decrease may be due to the diamagnetism of the new magnetosheath plasma being injected into the tail by the FTEs.

Citation: Slavin, J. A., et al. (2012), MESSENGER observations of a flux-transfer-event shower at Mercury, *J. Geophys. Res.*, *117*, A00M06, doi:10.1029/2012JA017926.

1. Introduction

[2] The MErcury Surface, Space ENvironment, GEochemistry, and Ranging (MESSENGER) spacecraft entered orbit about Mercury on 18 March 2011 [*Solomon et al.*, 2007]. Projections of MESSENGER's 82° inclination, highly eccentric (~200 × 15,200 km altitude) orbit onto a noon–midnight meridional cross section through Mercury's magnetosphere are depicted in Figure 1 [*Zurbuchen et al.*, 2011]. The solid and dashed green ellipses correspond to the spacecraft's "warm" and "hot" seasons when periapsis is on the nightside or dayside, respectively. As shown, these orbits tend to skim the magnetopause on the dayside, and the spacecraft enters and exits the nightside magnetotail along quasi-perpendicular trajectories downstream of the southern magnetospheric cusp.

[3] The MESSENGER magnetic field measurements [*Anderson et al.*, 2007] show that Mercury's magnetic field is largely dipolar with the same polarity as at Earth, but the dipole moment is closely aligned with the planetary rotation axis and offset northward from the center of the planet by 484 km [*Anderson et al.*, 2008, 2011; *Alexeev et al.*, 2010]. In addition to acquiring observations of the magnetic field,

[1]Department of Atmospheric, Oceanic and Space Sciences, University of Michigan, Ann Arbor, Michigan, USA.
[2]Department of Physics and Astronomy, University of Leicester, Leicester, UK.
[3]Heliophysics Science Division, NASA Goddard Space Flight Center, Greenbelt, Maryland, USA.
[4]Goddard Earth Sciences and Technology Center, University of Maryland, Baltimore County, Baltimore, Maryland, USA.

Corresponding author: J. A. Slavin, Department of Atmospheric, Oceanic and Space Sciences, University of Michigan, Rm. 1517, Space Research Bldg., 2455 Hayward St., Ann Arbor, MI 48109–2143, USA. (jaslavin@umich.edu)

0148-0227/12/2012JA017926

[5]Johns Hopkins University Applied Physics Laboratory, Laurel, Maryland, USA.
[6]Department of Earth and Ocean Sciences, University of British Columbia, Vancouver, British Columbia, Canada.
[7]Planetary Science Institute, Tucson, Arizona, USA.
[8]Solar System Exploration Division, NASA Goddard Space Flight Center, Greenbelt, Maryland, USA.
[9]Department of Terrestrial Magnetism, Carnegie Institution of Washington, Washington, D. C., USA.
[10]Lamont-Doherty Earth Observatory, Earth Institute at Columbia University, Palisades, New York, USA.

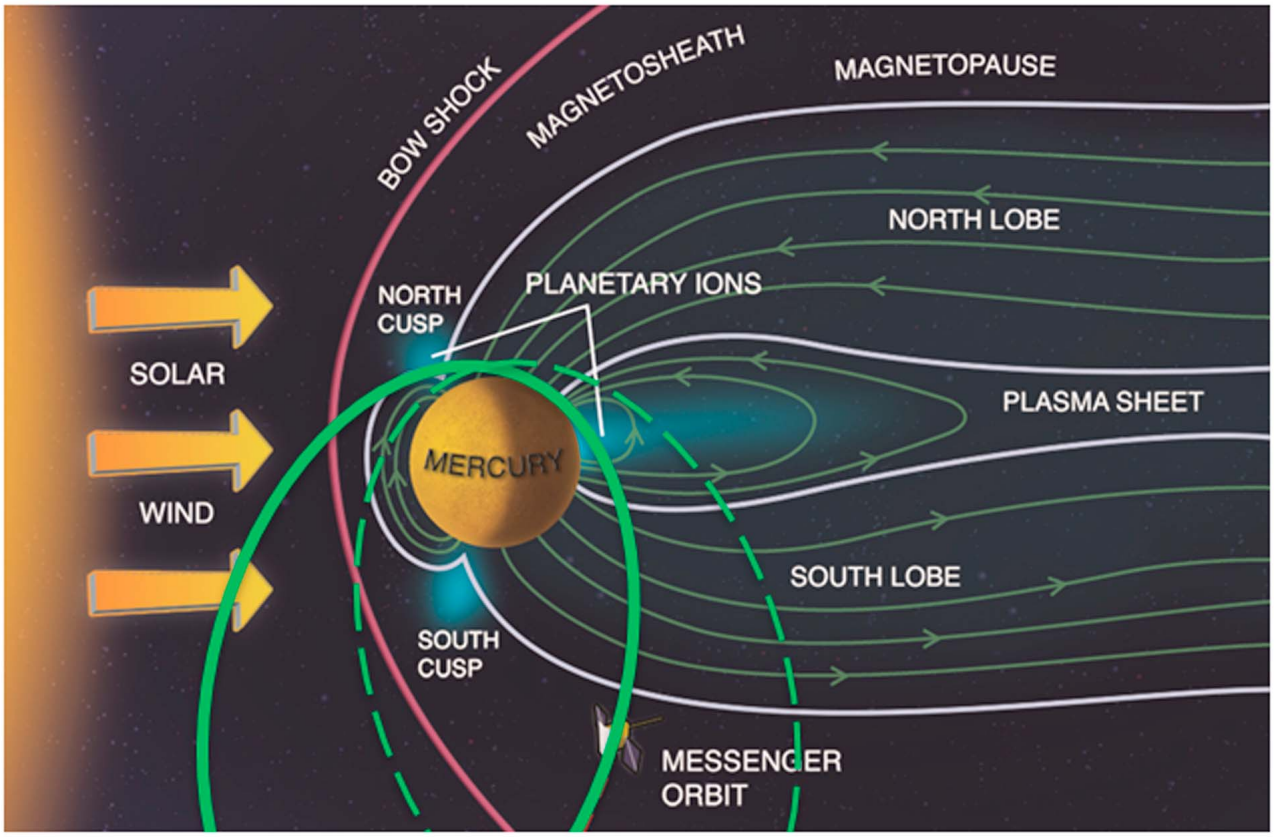

Figure 1. MESSENGER orbits with periapsis at local noon (dashed green ellipse) and local midnight (solid green ellipse) are displayed against a schematic cross section of Mercury's magnetosphere, with the Sun at left (adapted from *Zurbuchen et al.* [2011]).

MESSENGER measures the distribution and mass per charge of thermal ions at energies up to 13 keV with its Fast Imaging Plasma Spectrometer (FIPS), but the orientation of the spacecraft and shadowing by the spacecraft's sunshade allow direct observations of the solar wind only under limited conditions [*Zurbuchen et al.*, 2011].

[4] At Earth, magnetic reconnection occurs with increasing frequency and intensity as the shear angle across the magnetopause increases from small values (i.e., "component" reconnection) toward 180° (i.e., "antiparallel" reconnection) [*Sonnerup*, 1974; *Fuselier and Lewis*, 2011]. The rate of reconnection at Mercury's magnetopause is much greater than at Earth, and its role in magnetospheric dynamics is correspondingly stronger [*Slavin et al.*, 2009, 2010]. The reason for the high rate of reconnection is thought to be the strong interplanetary magnetic field (IMF) and low Alfven Mach number and low values of plasma β, the ratio of plasma thermal pressure to magnetic pressure, in the inner solar system [*Slavin and Holzer*, 1979].

[5] Magnetic reconnection at the dayside magnetopause breaks "closed" magnetic field lines having both ends rooted in Mercury and creates a pair of "open" field lines with one end connected to the IMF. As depicted in Figure 2a, these newly opened magnetic field lines are rapidly pulled antisunward by the solar wind flow in the magnetosheath and added to the open magnetic flux in the northern and southern lobes of the magnetotail. In this manner, they drive the circulation of magnetic flux and plasma that constitutes the Dungey cycle [*Dungey*, 1961].

[6] When the IMF has a northward tilt, reconnection can occur not only at the forward magnetopause, but also just tailward of the northern and southern magnetic cusps. However, this high-latitude reconnection does not add any net magnetic flux to the tail. As shown in Figure 2b, this reconnection between the IMF and the lobe magnetic field strips existing open field lines out of the tail lobes and promptly replaces them with a new field line that is swept into the tail by pivoting about the end anchored in the cusp. In doing so, high-latitude reconnection is adding to the lobe region a field line carrying magnetosheath plasma, which will continue to move tailward while $\mathbf{E} \times \mathbf{B}$ drifting toward the plasma sheet under the influence of the dawn-to-dusk magnetospheric electric field $\mathbf{E}$ (where $\mathbf{B}$ is the vector magnetic field).

[7] Continued reconnection at an extended, dayside X line produces a normal magnetic field over a broad region of the Earth's magnetopause downstream of the reconnection site [*Fuselier and Lewis*, 2011]. However, discrete bundles of twisted open magnetic flux called flux transfer events (FTEs) form with one end connected to the geomagnetic field and the other to the IMF [*Russell and Elphic*, 1978]. As shown in Figures 3a and 3b [*Fear et al.*, 2007], the outer layers of FTEs have a helical topology that winds magnetic flux about an axial magnetic field near the center of the structure. The axial "core" field in these FTE-type flux ropes

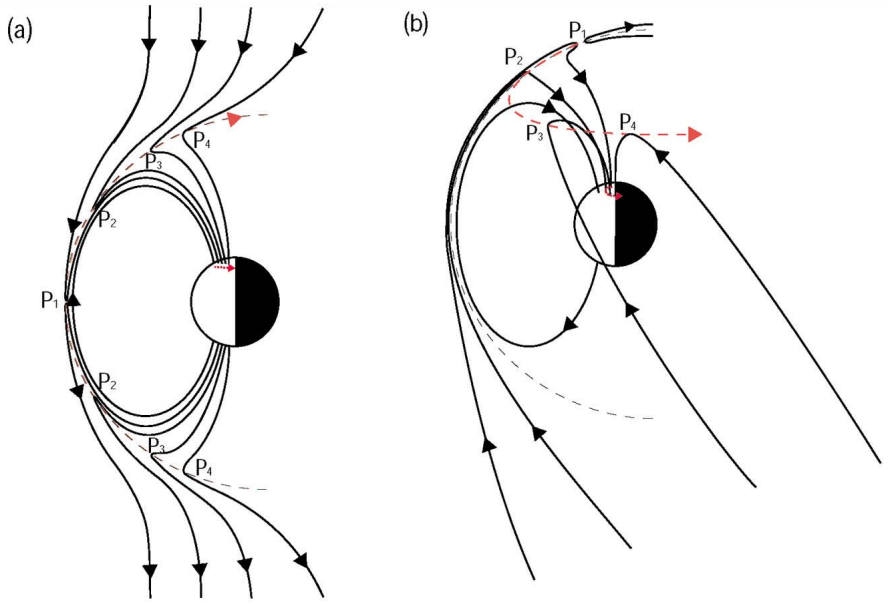

Figure 2. The motion of open planetary field lines (black lines with arrows) due to (a) a southward and (b) a northward IMF. The sense of motion of the feet of the field lines on the planet is shown by small red arrows. In Figure 2a, open magnetic field lines are created by low-latitude dayside reconnection between the IMF and the planetary magnetic field, starting at time P_1 and progressing through time P_4 as the lines are transported antisunward and added to the tail. In Figure 2b, new open magnetic field lines created by reconnection just tailward of the northern magnetic cusp at time P_1 move and progress through time P_4 as the lines pivot about the cusp and are transported into the tail.

is then compressed and amplified by the tension in those outer layers [*Russell and Elphic*, 1978]. FTEs with their characteristic flux rope structure are believed to form as a result of simultaneous reconnection at two or more X lines at the magnetopause, as shown in Figures 3c and 3d [*Lee and Fu*, 1985; *Zong et al.*, 2005; *Raeder*, 2006; *Fear et al.*, 2007; *Hasegawa et al.*, 2008, 2010; *Trenchi et al.*, 2011]. The FTEs are then carried tailward by the solar wind flow in the magnetosheath and added to the tail, as shown in Figure 2a.

[8] When spacecraft pass through FTEs, such events are identified directly by their flux rope structure [*Wang et al.*, 2005]. Alternatively, when the observing spacecraft passes near but does not enter the FTE, the characteristic draping and compression of the surrounding magnetic flux as the FTE moves tailward may be used infer its passage and approximate dimensions. These magnetic field perturbations are termed FTE-type traveling compression regions (TCRs) [*Liu et al.*, 2008].

[9] Flux transfer events at Mercury were first identified in the Mariner 10 flyby magnetometer observations and analyzed by *Russell and Walker* [1985]. Initial examinations of the MESSENGER magnetic field measurements confirmed the presence of FTEs [*Slavin et al.*, 2008]. Subsequent analyses revealed that they are larger, both in diameter and axial magnetic flux content, relative to Mercury's magnetosphere than FTEs at Earth [*Slavin et al.*, 2010]. Here we present the first observations of FTEs at Mercury during MESSENGER's orbital mission phase. When MESSENGER passes through the outer layers of the southern tail lobe and exits into the magnetosheath near the noon–midnight meridian, it is well positioned to observe FTEs moving tailward after forming near the southern cusp. These MESSENGER magnetic field measurements often show the quasiperiodic occurrence of FTEs ~2–3 s in duration and spaced in time at intervals of ~8–10 s. No solar wind or magnetosheath plasma velocity measurements are available for the orbital observation intervals examined in this study. For this reason we rely on averages or numerical models of plasma flow speed in the analysis of MESSENGER magnetic field observations of flux transfer events. On the basis of these analyses, we suggest that flux transfer events are major contributors of solar wind energy and plasma to Mercury's magnetosphere.

2. FTE Shower of 11 April 2011

[10] MESSENGER Magnetometer measurements taken during a typical magnetospheric passage on 11 April 2011, when the IMF was predominantly northward, are shown in Figure 4. The inbound magnetopause crossing occurred at ~04:07:53 Coordinated Universal Time (UTC) at a magnetic latitude of ~81° and an altitude of 954 km, or 0.39 R_M (where R_M is Mercury's radius or 2440 km) in the prenoon sector as the spacecraft moved northward and antisunward through the outer portion of the southern magnetospheric cusp. The magnetic field is displayed in Mercury solar orbital (MSO) coordinates, in which X is oriented from the center of Mercury toward the Sun, Y is in the plane of Mercury's orbit and positive in the direction opposite to planetary motion, and Z completes the right-handed system.

[11] The magnetosphere during this passage was in a relatively quiet state similar to that observed during the first MESSENGER flyby [*Slavin et al.*, 2008]. Mercury was in an

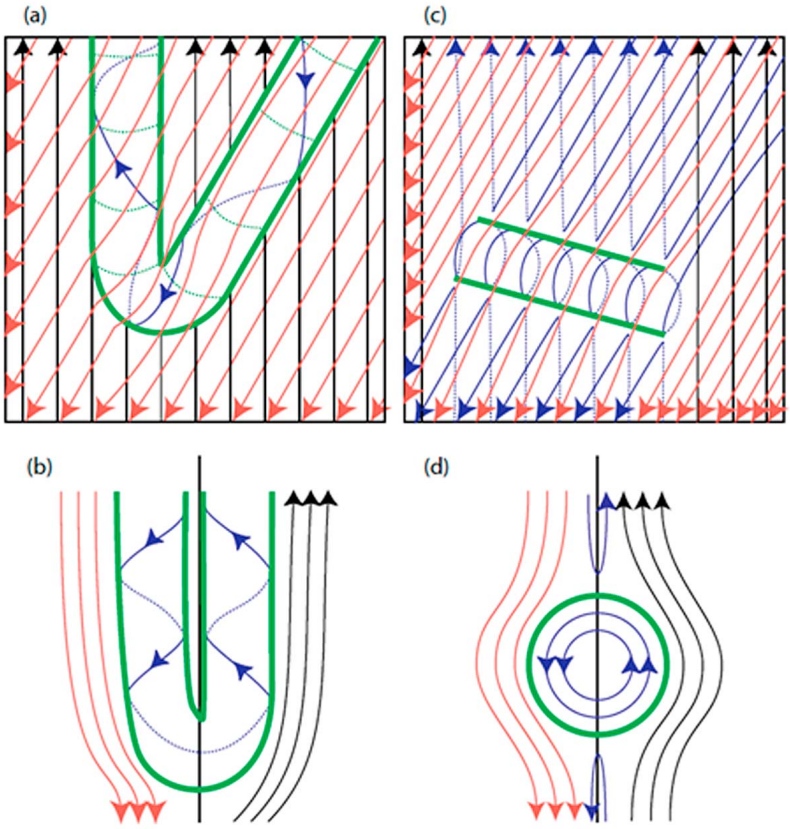

Figure 3. (a) Flux transfer event viewed against the surface of the magnetopause with the right-hand side of the twisted flux tube connected to the draped IMF in the magnetosheath and pulled upward (antisunward). Red lines are draped magnetosheath field lines. Black lines are magnetospheric field lines. New open field lines created by reconnection and having one end connected to the IMF and the other end to the planet are shown in blue. Green lines mark the boundary of the flux-rope–type FTE. (b) Side view of the same event as in Figure 3a with the right-hand side (left-hand side) of the flux tube inside the magnetosphere (magnetosheath). (c) Flux transfer event viewed against the surface of the magnetopause just after it formed as a result of simultaneous reconnection at two X lines. (d) Side view of the same event as in Figure 3c with the right-hand side (left-hand side) of the flux tube inside of the magnetosphere (magnetosheath) (adapted from *Fear et al.* [2007]).

inward ($B_X > 0$ and $B_Y < 0$) IMF sector and B_Z was > 0. Little or no diamagnetic depression of the magnetic field was observed in the region of the nightside plasma sheet [*Korth et al.*, 2011] as the spacecraft moved southward through the magnetic equatorial plane and entered the southern lobe of the magnetotail. MESSENGER then continued down through the southern lobe, crossed the magnetopause around 05:16:30 UTC, and entered into the magnetosheath.

[12] A close-up of MESSENGER's trajectory on 11 April 2011 near the outbound magnetopause is displayed in Figure 5a relative to mean bow shock and magnetopause surfaces, according to the model of *Moldovan et al.* [2011]. As shown, MESSENGER started the interval in the southern lobe of the magnetotail before crossing the magnetopause and passing into the magnetosheath very near the solar wind aberrated noon–midnight meridional plane. The MESSENGER magnetic field measurements for this interval are plotted in Figure 5b. The strong, relatively steady, low-variance magnetic fields oriented largely away from the planet indicate that the spacecraft remained in the southern lobe of the tail until ~05:16:30 UTC. The magnetosheath region displayed variable-direction, high-variance magnetic fields that persisted for the rest of the interval.

[13] The 163 flux transfer events identified in this 25 min interval are marked by vertical arrows in Figure 5b. The first 97 FTEs were detected on the basis of the traveling compression region perturbations generated as the TCRs moved tailward along the magnetopause boundary [*Owen et al.*, 2008; *Liu et al.*, 2008]. The flux ropes that form in the magnetopause current sheet, as shown in Figure 3, are pushed against the magnetopause by the solar wind flow in the magnetosheath, depress the magnetopause, and compress the lobe magnetic field. As a flux rope in the magnetosheath moves tailward, the compression "travels" and causes the lobe magnetic field to tilt in and out relative to the magnetopause normal direction as the compression moves over and past the spacecraft. A schematic view of this interaction between the flux ropes created by reconnection at the cusp and the southern lobe is shown in Figure 6a.

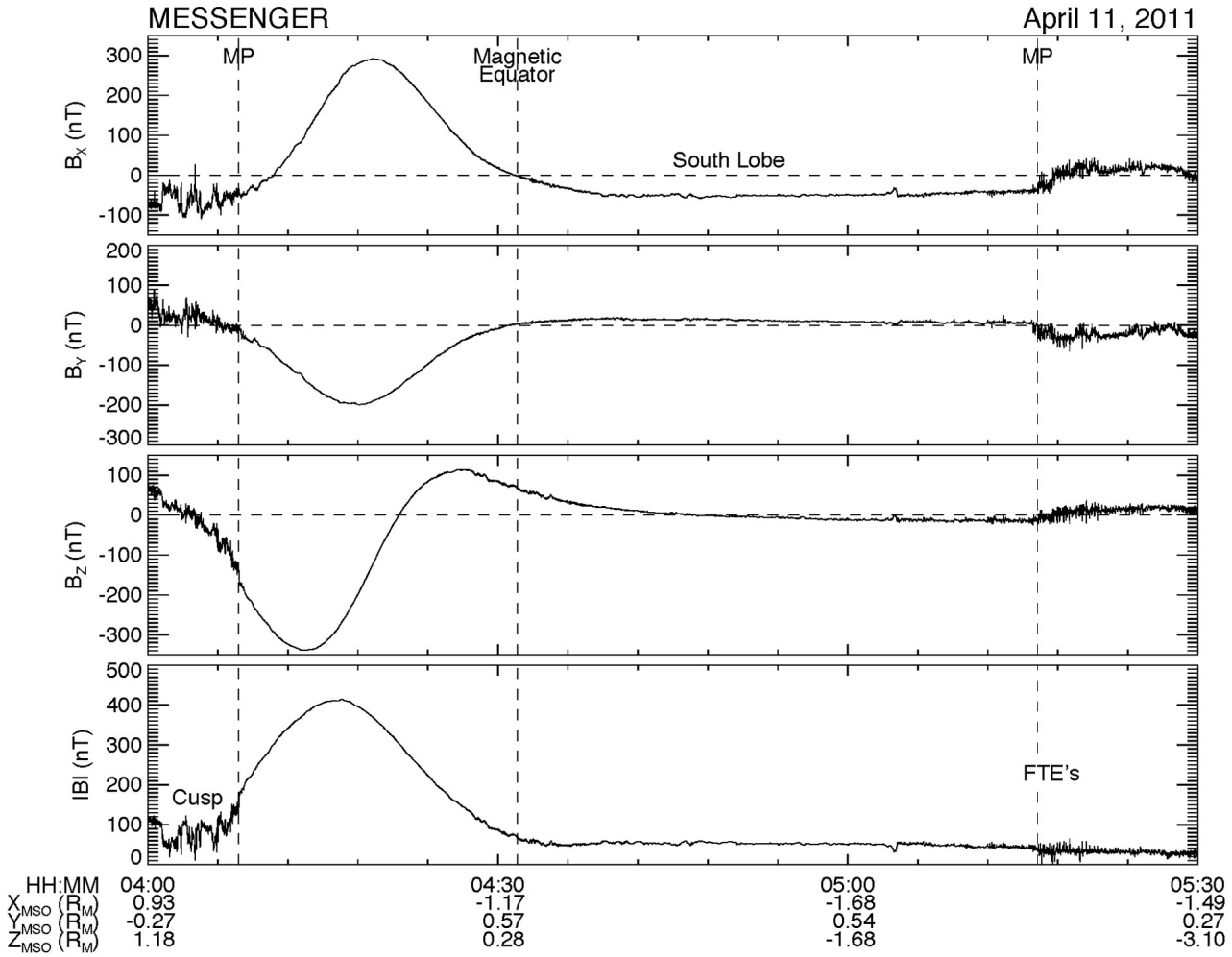

Figure 4. Magnetic field measurements (at a sampling rate of 20 s^{-1}) taken during a magnetospheric pass on 11 April 2011, displayed in MSO coordinates. The inbound magnetopause crossing is marked with the vertical dashed line on the left. The crossing of the nightside magnetic equator is marked by the transition in the B_X component from >0 (northern hemisphere) to <0 (southern hemisphere) and the vertical dashed line in the center. After MESSENGER transited the southern lobe of the tail, it exited the magnetosphere through the magnetopause (vertical dashed line on the right) and entered the magnetosheath.

[14] Another 66 FTEs were then observed directly on the basis of their flux rope signatures in the magnetic field data after MESSENGER entered the magnetosheath. The large-amplitude increases in the total magnetic field that mark their presence in Figure 5b are due to MESSENGER passing through their high-intensity core magnetic fields [*Slavin et al.*, 2009, 2010]. We term the extended interval with quasiperiodic FTE-type TCRs and flux ropes in the magnetic field measurements an "FTE shower." Some TCRs and flux ropes are present in the data collected before and after the 25 min long shower shown in Figure 5. Those earlier and later events, however, occurred on a sporadic basis with very irregular temporal separation and are not considered here as part of the FTE shower.

[15] To better examine the FTE-type TCR and flux rope signatures present in the MESSENGER showers, two 1 min intervals of magnetic field measurements taken just before and after the magnetopause crossing are presented in Figures 6b and 6c. Both types of FTE signatures are best identified by examining the high-time-resolution magnetic field measurements in a local boundary-normal coordinate system [*Russell and Elphic*, 1978]. The boundary normal can be determined either on the basis of an average magnetopause model or minimum variance analysis of the magnetopause. In Figures 6b and 6c the magnetic field measurements are displayed in boundary-normal coordinates determined from minimum variance analysis of the magnetopause (MP) current sheet: B_1 is the component in the direction of minimum variance (positive outward from the MP), which corresponds to the boundary normal direction; B_2 and B_3 are the components in the directions of intermediate and maximum variance, respectively. Vertical dashed lines mark each of the FTEs in Figures 6b and 6c. The lobe FTE-type TCRs consist of several-seconds-long compressive perturbations with the $\pm B_1$ normal field variation signaling their tailward motion [*Russell and Elphic*, 1978; *Russell and Walker*, 1985, *Wang et al.*, 2005]. FTE-type flux ropes (Figure 6c) observed several minutes later are identified by the $\pm B_1$ perturbation indicating tailward motion and their associated unipolar core

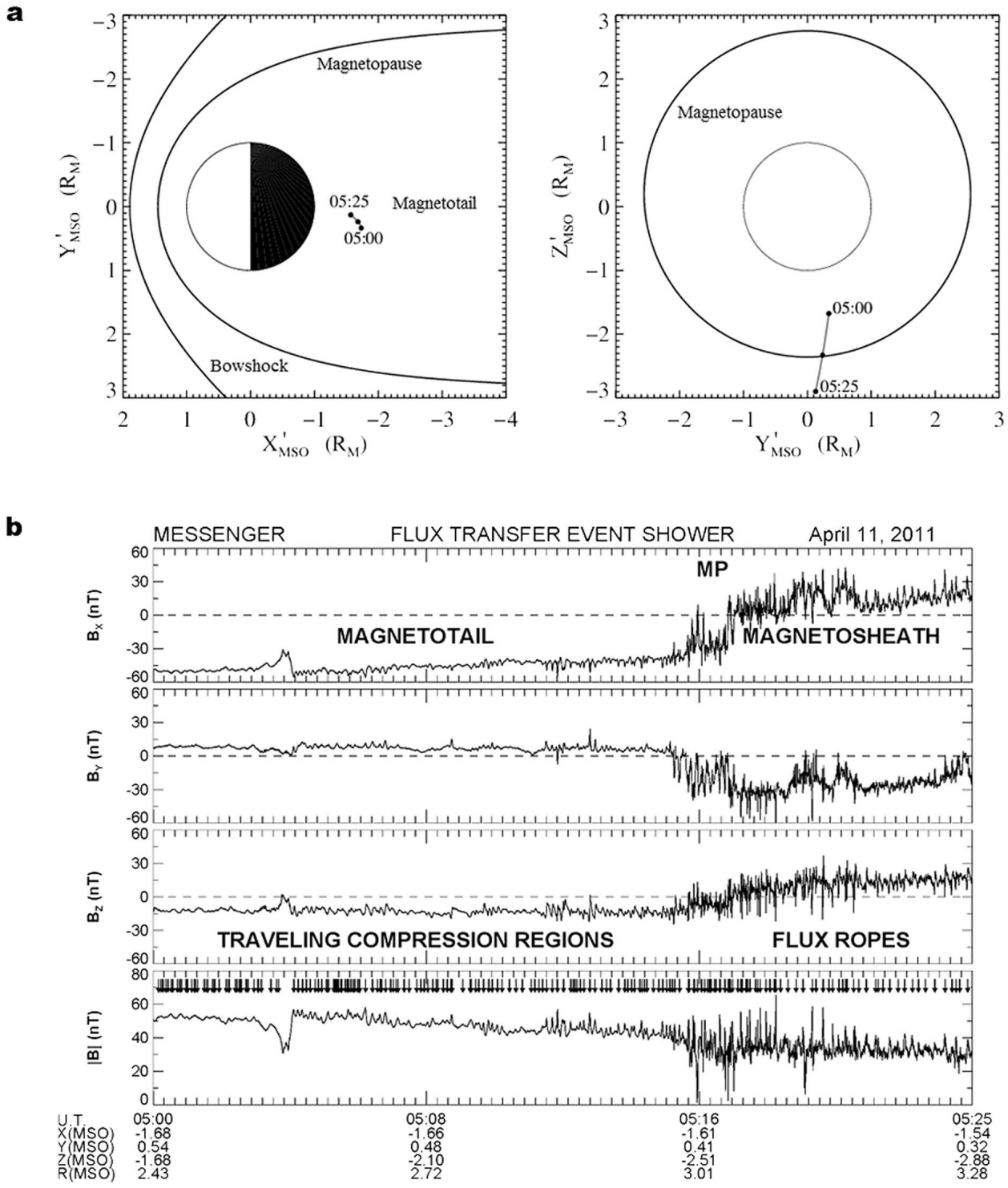

Figure 5. (a) MESSENGER trajectory from 05:00 to 05:25 UTC on 11 April 2011, projected onto the aberrated MSO *X–Y* and *Y–Z* planes. Note that the bow shock and magnetopause surfaces are shifted northward by 0.20 R_M to match the northward offset in Mercury's internal magnetic dipole. (b) Magnetic field measurements taken during this interval span the outer portion of the southern lobe of Mercury's magnetotail, the magnetopause, and the nearby magnetosheath. Vertical arrows in the fourth panel mark 97 TCRs inside the magnetotail and 66 FTE-type flux ropes in the adjacent magnetosheath.

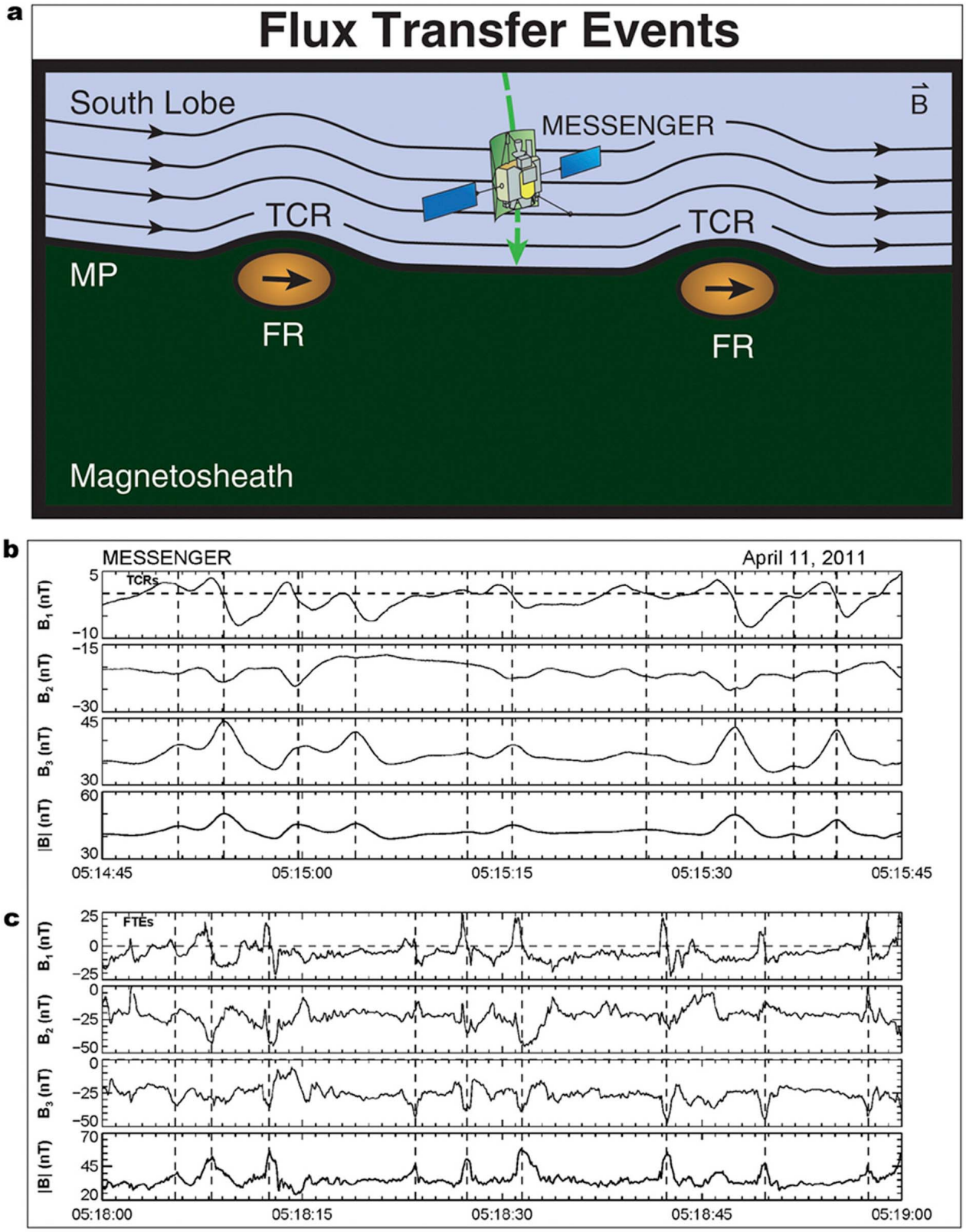

Figure 6. (a) Schematic view of FTE-type TCRs and flux ropes passing over the MESSENGER spacecraft as it approached the magnetopause and then entered the magnetosheath. (b and c) Magnetic field measurements at 1 min intervals just inside and outside of the magnetopause; the TCRs and FTEs are marked with vertical dashed lines. The unit eigenvectors from minimum variance analysis in MSO coordinates are B_1 = (0.34, −0.02, −0.94), B_2 = (0.57, 0.81, 0.19), and B_3 = (−0.76, 0.59, −0.29).

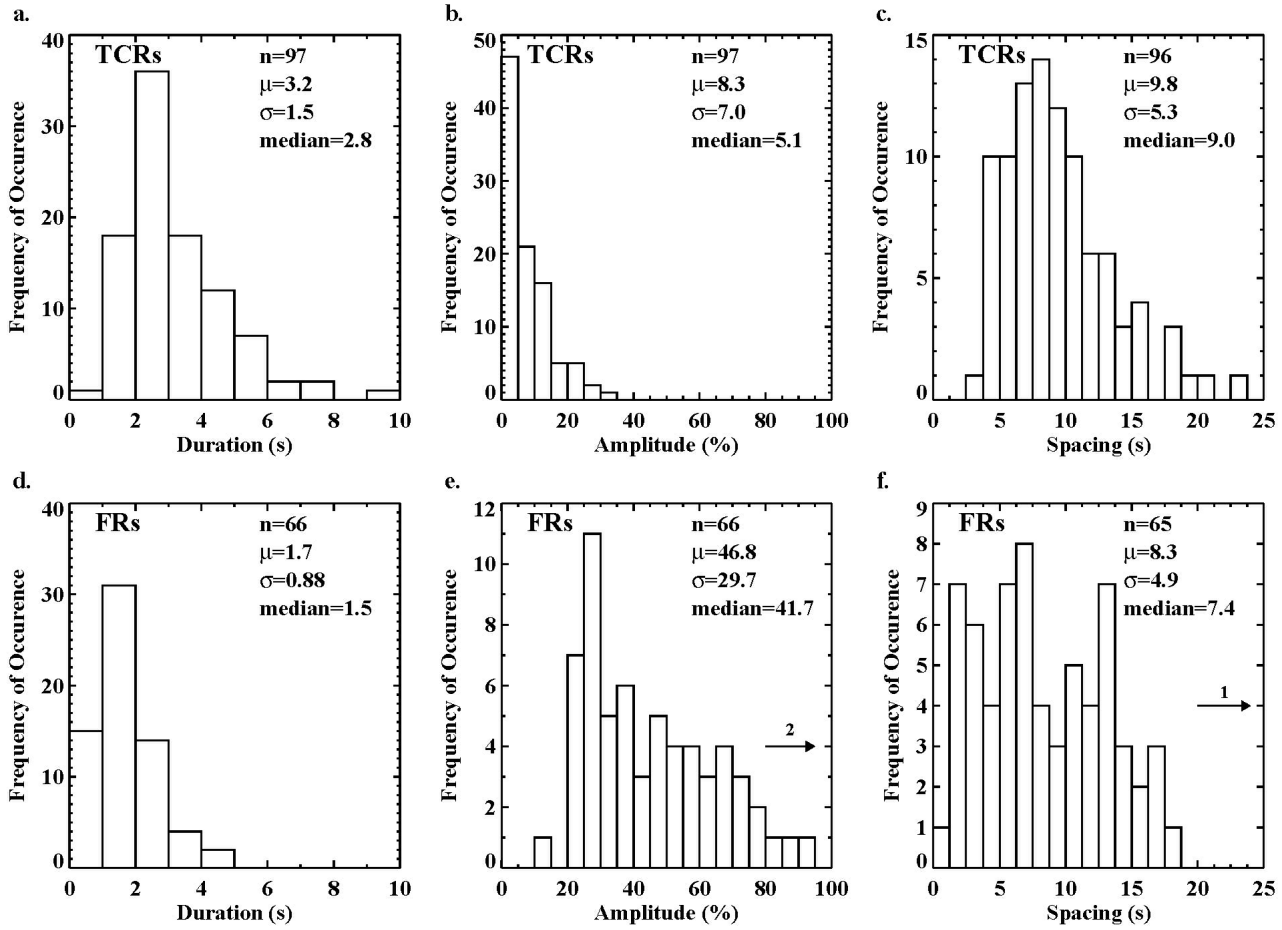

Figure 7. Histograms of the (a) duration of, (b) amplitude of, and (c) temporal spacing between TCRs along with the number, *n*, mean, μ, standard deviation, σ, and median for each distribution. (d–f) Same as Figures 7a–7c but for the flux ropes (FRs).

field [*Moldwin et al.*, 2001; *Liu et al.*, 2008]. When minimum variance analysis is performed on individual flux ropes, the unipolar core field increase appears in the B_2 direction as expected [*Russell and Elphic*, 1978]. In contrast, the core fields in Figure 6c appear in either B_2 or B_3 because of differences in the orientations of individual flux ropes and the single coordinate system defined from minimum variance analysis of the magnetopause field. The similarities in the temporal spacing and duration of the TCRs and flux ropes argue strongly for their causal linkage.

3. FTE-Type Flux Rope and TCR Properties

[16] For each of the FTE-type flux ropes and TCRs identified in the shower of 11 April 2011, the duration of the events was determined from the extrema in the $\pm B_1$ variation. The amplitude, $\Delta B/B$, of the peak variation in magnetic field magnitude relative to the mean magnetic field before and after the flux rope or TCR, respectively, was measured. The spacing between successive FTEs was also determined for each flux rope and TCR. The results are displayed as histograms in Figures 7a–7f.

[17] The lobe TCRs have a mean duration of 3.2 s, a mean relative amplitude of 8.3%, and a mean spacing between events of 9.8 s. The flux ropes have a mean duration of 1.7 s, a mean relative amplitude of 46.8%, and a mean spacing of 8.3 s. The somewhat greater duration of the compression regions relative to the flux ropes that produce them is due to magnetic field line tension causing the lobe field to "tent" about the inward deformation of the magnetopause caused by the tailward moving flux rope. This effect has been previously observed for TCRs generated at Earth by the interaction of plasmoid-type flux ropes with the lobes as they are ejected down the tail [*Slavin et al.*, 1993]. The mean amplitude of the magnetosheath flux ropes is comparable to the strong core magnetic fields observed when spacecraft penetrate into the central region of FTE-type flux ropes near Earth [*Zhang et al.*, 2008]. The mean spacing between adjacent TCRs and flux ropes is the same to within the statistical errors at 9.8 s and 8.3 s, respectively.

4. Flux Rope Modeling

[18] In order to determine the cross-sectional shape, area, and magnetic flux content of the FTE-type flux ropes in this shower event, we modeled them using the method developed by *Hidalgo et al.* [2002a, 2002b]. This model has been used to determine the magnetic flux rope topology of the magnetic clouds embedded in coronal mass ejections in the interplanetary medium. The model begins with an assumed flux rope

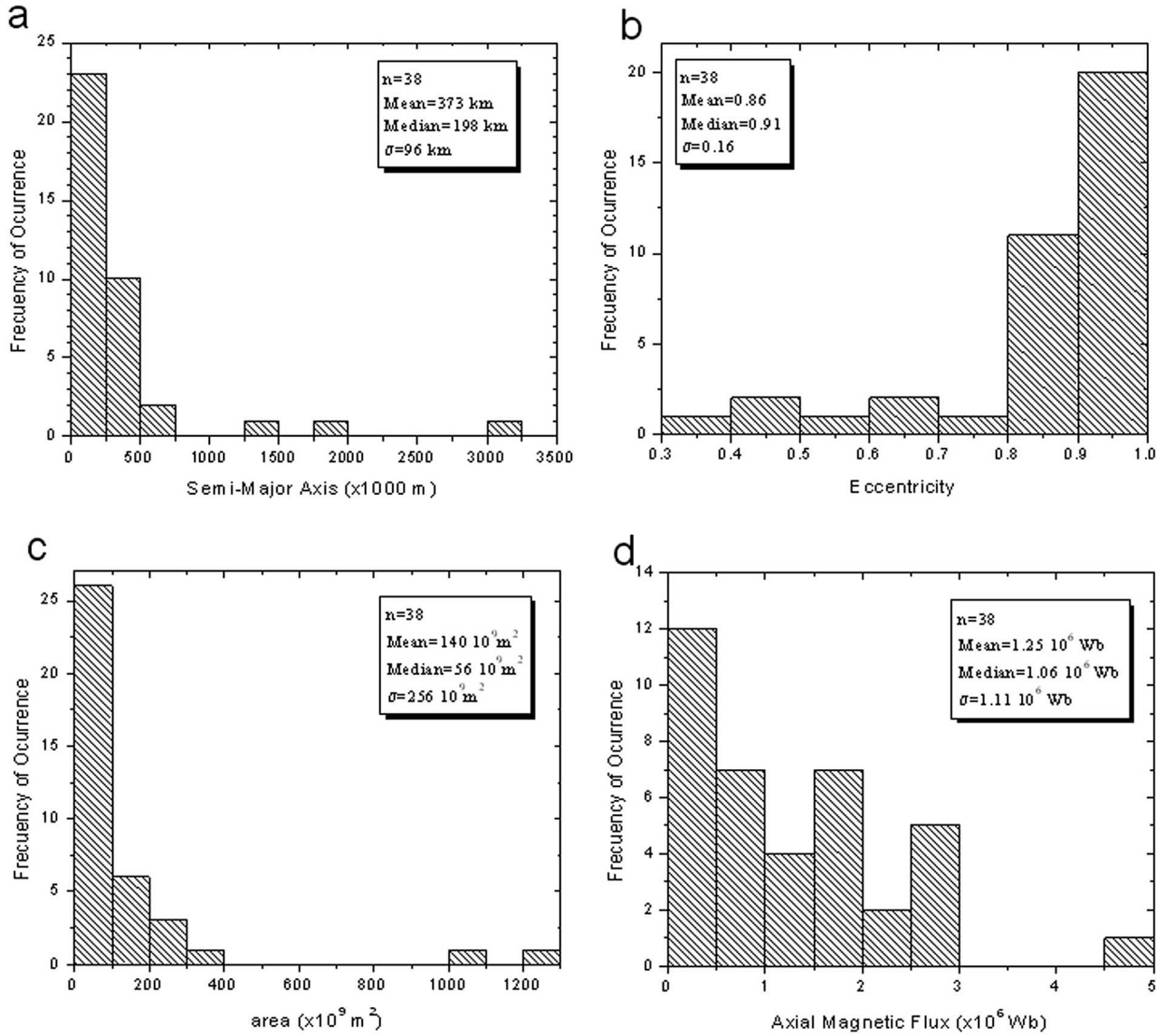

Figure 8. Flux rope properties determined for the 38 events that were well described by the *Hidalgo et al.* [2002a] model: (a) semimajor axis; (b) eccentricity; (c) cross-sectional area; and (d) axial magnetic flux.

magnetic field topology and treats separately the radial and axial electric currents, avoiding any force-free restriction. The local solutions of Maxwell's equations in elliptic-cylindrical coordinates provide the three magnetic field components, which are then transformed into spacecraft coordinates. The only assumptions are that the radial and axial components of the current density are constant and the value of the unmeasured magnetosheath flow speed. Note that the cross section of the flux ropes is not required to be circular. At the downstream location where MESSENGER crossed into the magnetosheath, the magnetosheath flow speed is predicted by numerical flow models to be ~90–95% of the upstream solar wind speed [*Spreiter et al.*, 1966]. For this reason we assumed that these FTE-type flux ropes moved over the spacecraft with a mean speed of 400 km/s. The ellipticity of the flux rope cross section, the current density components, the axial magnetic field, and the spacecraft trajectory relative to the flux rope were determined by fitting the magnetic field data. The fitting process began with a minimum variance technique to produce initial estimates of the flux rope orientation. Multiple regression analysis was then used to infer the spacecraft trajectory through the flux rope. Current density components, the cross section ellipticity and dimensions, and the flux rope orientation are output parameters in the fitting procedure.

[19] For a fit to be accepted the procedure must converge, and a high degree of correlation between model and data must be obtained (i.e., events with correlation coefficients lower than 0.99 are discarded as "irregular"). Further details concerning the fitting algorithm were given by *Hidalgo et al.* [2002a, 2002b]. Possible causes for the lack of convergence in the fitting procedure for a given FTE include, for example, ambiguity in the choice of the boundaries, errors in our assumption of a constant 400 km/s speed for the magnetosheath flow in which the FTE is embedded, or spacecraft trajectories through the flux rope that did not pass close to

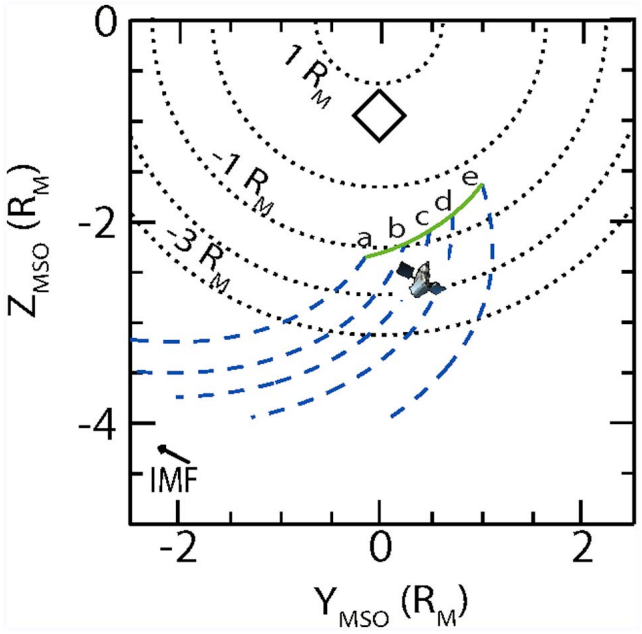

Figure 9. Cooling model predictions of FTE motion at Mercury in the MSO *Y–Z* plane for the 11 April 2011 shower. The dotted circles cut through the magnetopause at constant *X*, and a diamond marks the southern cusp. The blue dashed lines show the trajectories of reconnected flux tubes that are launched along the X line indicated by the green curve. The location of MESSENGER at the time of the FTE observations is also shown.

the center of the structure and limited the portion of the flux rope sampled by the spacecraft.

[20] The 38 flux ropes observed by MESSENGER on 11 April 2011 for which satisfactory model fits were obtained are displayed in Figure 8. The mean semimajor axis for these flux ropes, displayed in Figure 8a, was 373 km or 0.15 R_M. In Figure 8b, the distribution of eccentricities is shown. The mean value of 0.86, given that an eccentricity of 0 is a circle and 1 is a parabola, indicates that the FTE flux ropes were indeed flattened by their pushing up against the magnetopause (Figure 6a). The mean values of the cross-sectional area and magnetic flux content, displayed in Figures 8c and 8d, were 1.4×10^{11} m^2 and 1.25 MWb, respectively. By comparison, the inferred axial magnetic contents of the six equatorial FTEs observed during the flybys and analyzed by *Slavin et al.* [2010] with a cylindrical flux rope model [*Lepping et al.*, 1990] ranged from 0.001 to 0.2 MWb. As shown in Figure 8d, the most common axial magnetic flux contents for the high-latitude FTEs analyzed here were in this same range, but with a smaller number of events with fluxes up to ~5 MWb (Figure 8).

5. Cooling Model for the FTE Shower of 11 April 2011

[21] The northward/sunward orientation of the IMF at the time of these FTEs strongly suggests that they were formed at the southern cusp (see Figure 2) and then moved tailward to pass over MESSENGER. This scenario was tested with a magnetohydrodynamic model of FTE motion in response to the solar wind and the magnetic forces resulting from its connection to the IMF [*Cooling et al.*, 2001]. The Cooling model was first developed to predict the motion of flux tubes formed by reconnection either at low latitudes or just poleward of the cusp at Earth [*Cooling et al.*, 2001]. For our calculation, the magnetosheath magnetic field and the paraboloid shape of the magnetopause were defined with the model of *Kobel and Flückiger* [1994]. The magnetosheath flow and density were derived from the gasdynamic models of *Spreiter et al.* [1966]. Geomagnetic field lines just inside the magnetopause map from the southern to the northern cusp to encompass the surface of the magnetopause. The probability of reconnection taking place at a given location on the magnetopause was calculated as a function of solar wind input conditions with a component reconnection model proposed by *Crooker* [1979]. The reconnected flux tubes were then traced along the magnetopause according to *Cowley and Owen* [1989] on the basis of the stress on the flux tube due to the sheath flow and the magnetic tension on the field line. We have adapted this model to Mercury within the constraints of the MESSENGER data set. For this reason, mean values of solar wind parameters were assigned, but the IMF values were estimated from magnetosheath data. With this model we predicted the location, orientation, and velocity of FTEs generated by reconnection at the magnetopause.

[22] We have applied the Cooling model of FTE motion to the 11 April 2011 shower event to confirm that FTEs formed just tailward of the southern magnetic cusp would indeed intercept the MESSENGER spacecraft. Figure 9 shows the southern portion of the magnetopause, as viewed from the Sun, with dashed circles representing contours of constant MSO *X* and a diamond marking the location of the southern cusp. The magnetopause was modeled as a paraboloid and scaled to match the location of the outbound magnetopause crossing. Reconnection was initiated along a line of maximum shear between the sheath and planetary field, centered at a point on the magnetopause given by [−0.8, 0.5, −2.1] (R_M). The X line was extended 1.5 R_M in length from this point, and five FTE flux tubes were launched at equal intervals along its length. Solar wind conditions were set to typical values of 400 km/s velocity and 73 cm^{-3} density. The model traces the intersection of the newly created flux tubes and the magnetopause for 100 s, as shown by the blue dashed lines. All of the five flux tubes are connected to the southern hemisphere. FTEs created along an extended X line near the southern magnetic cusp would indeed be expected to be intercepted by MESSENGER on 11 April 2011 for any foreseeable set of assumptions regarding solar wind and IMF conditions.

6. Discussion and Summary

[23] During the MESSENGER flybys, flux transfer events were observed along the spacecraft's near-equatorial trajectories following intervals of IMF $B_Z < 0$ [*Slavin et al.*, 2010]. Here we have presented the first observations of quasiperiodic FTE occurrence downstream of the southern magnetic cusp. MESSENGER's orbit is especially well suited to observe these high-latitude "FTE showers." Statistical studies still remain to be carried out, but intervals of quasiperiodic FTEs appear quite common in the Magnetometer data, particularly

when IMF $B_X > 0$ and $B_Z > 0$. During the 11 April 2011 shower examined here, 163 FTEs were identified within a duration of 25 min from magnetic field measurements. Had MESSENGER's orbit not carried the spacecraft away from the magnetopause, the shower presumably would have continued until the upstream IMF conditions changed.

[24] The strong interaction between the high-latitude FTEs and the magnetopause reported here from orbital measurements led us to apply a flux rope model that included elliptical cross sections to account for flattening of the flux ropes [*Hidalgo et al.*, 2002a, 2002b]. Indeed, the results indicated that these high-latitude FTEs do generally have elliptical cross sections, implying substantial flattening by their interaction with the flanks of the magnetopause and yielding a mean semimajor axis of 373 km. Further, the modeling is generally consistent with the earlier analyses [*Slavin et al.*, 2009, 2010] of Mercury FTEs observed at low latitudes. From fits to a force-free flux rope model with a circular cross section, *Slavin et al.* [2009, 2010] determined flux rope radii of 0.1–0.5 R_M (i.e., 240–1200 km) and axial magnetic flux contents up to 0.2 MWb. The mean axial flux content of the FTEs determined here for high-latitude flux ropes with an elliptical cross-sectional model was substantially larger, 1.25 MWb. In the absence of in situ measurements of the speed with which the MESSENGER FTEs moved past the spacecraft, the largest values inferred for the diameter and axial flux contents of these Mercury FTEs must be considered uncertain by at best a factor of ~2. However, the results of both modeling analyses indicate that FTE-type flux ropes can transport a quantity of magnetic flux comparable to the ~2 to 4 MWb contained in a single lobe of Mercury's tail [*Alexeev et al.*, 2010; C. L. Johnson et al., MESSENGER observations of Mercury's magnetic field structure, submitted to *Journal of Geophysical Research*, 2012] with as few as ~3 to 4 or as many as several tens of FTEs. Given our observations of FTE repeat times of only ~8 s and the ~2 min Dungey time for the circulation of plasma and magnetic flux within this magnetosphere [*Slavin et al.*, 2009], it appears that FTEs may be the primary driver for magnetospheric convection at Mercury. In contrast, FTEs at Earth have been observed to occur with a range of separations centered on ~8 min, they possess a typical radius normal to the magnetopause surface of ~0.5 R_E (i.e., ~3000 km), and a magnetic flux content of ~1 MWb [*Rijnbeek et al.*, 1984; *Hasegawa et al.*, 2006; *Zhang et al.*, 2008]. However, the Earth's magnetic tail has a mean magnetic flux content of ~8000 MWb and a Dungey cycle time of ~1 h. In contrast with Mercury, the ~8 FTEs occurring during an average Dungey cycle at Earth would transport magnetic flux comparable to only ~0.1% of the magnetic flux in one lobe of the tail. The size and relative impact of FTEs on Mercury's magnetosphere appears to be much greater than at Earth.

[25] The time intervals between FTEs at Mercury and Earth are even more disparate, with separations of ~8–10 s at Mercury and ~8 min at Earth [*Lockwood and Wild*, 1993]. One model for periodic FTE formation [*Raeder*, 2006] predicts that the time between successive FTEs increases linearly with magnetopause radius. However, the observed spacing between FTEs at Earth, ~8 × 60 s = 480 s, is greater than the 8 s determined at Mercury in this study by a factor of ~53 rather than the ratio of their magnetopause subsolar stand-off distances, ~20.

[26] Our observations and analysis strongly suggest that plasma conditions in the inner solar system are probably the dominant factors responsible for the great relative size and magnetospheric impact of FTEs at Mercury [*Kuznetsova and Zeleny*, 1986]. The influence of solar wind and IMF conditions on FTEs has been examined at Earth. Remarkably, *Wang et al.* [2005] did find that the duration of cusp FTEs at Earth and the temporal spacing between FTEs decreased as the intensity of the IMF increased and plasma β decreased. These empirical trends are supported by the MESSENGER observations of short-duration, closely spaced FTEs at Mercury, where the IMF magnitude is indeed much higher and the plasma β much lower than at 1 AU.

[27] The lobe magnetic field intensity in Figure 5b exhibits a steady decrease from a value of ~55 nT at the onset of the FTE-type TCRs to only ~40 nT just inside the magnetopause. This decrease in the intensity of the outer portions of the tail lobe magnetic field appears to be a common feature of FTE shower events. This decrease cannot be due to the decrease in the planetary dipole contribution to the tail field with increasing altitude, as the magnetic field in this region is due primarily to magnetospheric currents. For example, the contribution to the magnetic field from Mercury's internal dipole at MESSENGER at the beginning of the FTE shower in Figure 5 is only 5.8 nT, and it decreases to 3.4 nT at the magnetopause. However, high-latitude reconnection, and by extension high-latitude FTEs, is expected to transfer magnetosheath plasma into the magnetotail as older, plasma-depleted lobe flux tubes are replaced with newer, plasma-laden magnetosheath flux tubes [*Pilipp and Morfill*, 1978]. A portion of the magnetosheath ions added to the plasma mantle by these FTE showers will $\mathbf{E} \times \mathbf{B}$ drift into the plasma sheet sufficiently close to Mercury to be accelerated by tail reconnection events and impact the nightside of the planet. For this reason, high-latitude FTE plasma injection into the tail and subsequent acceleration should be examined to determine whether it could be an important source of neutral sputtering from Mercury's nightside surface.

[28] **Acknowledgments.** Computational assistance and data visualization support provided by J. Feggans are gratefully acknowledged. Discussion of the flux-transfer-event formation process with J. Raeder is also acknowledged. The MESSENGER project is supported by the NASA Discovery Program under contracts NASW-00002 to the Carnegie Institution of Washington and NAS5-97271 to the Johns Hopkins University Applied Physics Laboratory.

[29] Masaki Fujimoto thanks the reviewers for their assistance in evaluating this paper.

References

Alexeev, I. I., et al. (2010), Mercury's magnetospheric magnetic field after the first two MESSENGER flybys, *Icarus*, *209*, 23–39, doi:10.1016/j.icarus.2010.01.024.

Anderson, B. J., M. H. Acuña, D. A. Lohr, J. Scheifele, A. Raval, H. Korth, and J. A. Slavin (2007), The Magnetometer instrument on MESSENGER, *Space Sci. Rev.*, *131*, 417–450, doi:10.1007/s11214-007-9246-7.

Anderson, B. J., M. H. Acuña, H. Korth, M. E. Purucker, C. L. Johnson, J. A. Slavin, S. C. Solomon, and R. L. McNutt Jr. (2008), The structure of Mercury's magnetic field from MESSENGER's first flyby, *Science*, *321*, 82–85, doi:10.1126/science.1159081.

Anderson, B. J., C. L. Johnson, H. Korth, M. E. Purucker, R. M. Winslow, J. A. Slavin, S. C. Solomon, R. L. McNutt Jr., J. M. Raines, and T. H. Zurbuchen (2011), The global magnetic field of Mercury from MESSENGER

orbital observations, *Science*, *333*, 1859–1862, doi:10.1126/science.1211001.

Cooling, B. M. A., C. J. Owen, and S. J. Schwartz (2001), Role of the magnetosheath flow in determining the motion of open flux tubes, *J. Geophys. Res.*, *106*, 18,763–18,775, doi:10.1029/2000JA000455.

Cowley, S. W. H., and C. J. Owen (1989), A simple illustrative model of open flux tube motion over the dayside magnetopause, *Planet. Space Sci.*, *37*, 1461–1475, doi:10.1016/0032-0633(89)90116-5.

Crooker, N. U. (1979), Dayside merging and cusp geometry, *J. Geophys. Res.*, *84*, 951–959, doi:10.1029/JA084iA03p00951.

Dungey, J. W. (1961), Interplanetary magnetic field and the auroral zones, *Phys. Rev. Lett.*, *6*, 47–48, doi:10.1103/PhysRevLett.6.47.

Fear, R. C., S. E. Milan, A. N. Fazakerley, C. J. Owen, T. Asikainen, M. G. G. T. Taylor, E. A. Lucek, H. Rème, I. Dandouras, and P. W. Daly (2007), Motion of flux transfer events: A test of the Cooling model, *Ann. Geophys.*, *25*, 1669–1690, doi:10.5194/angeo-25-1669-2007.

Fuselier, S. A., and W. S. Lewis (2011), Properties of near-Earth magnetic reconnection from in-situ observations, *Space Sci. Rev.*, *160*, 95–121, doi:10.1007/s11214-011-9820-x.

Hasegawa, H., B. U. Sonnerup, C. J. Owen, B. Klecker, G. Paschmann, A. Balogh, and H. Rème (2006), The structure of flux transfer events recovered from Cluster data, *Ann. Geophys.*, *24*, 603–618, doi:10.5194/angeo-24-603-2006.

Hasegawa, H., A. Retinò, A. Vaivads, Y. Khotyaintsev, R. Nakamura, T. Takada, Y. Miyashita, H. Rème, and E. A. Lucek (2008), Retreat and reformation of X-line during quasi-continuous tailward-of-the-cusp reconnection under northward IMF, *Geophys. Res. Lett.*, *35*, L15104, doi:10.1029/2008GL034767.

Hasegawa, H., et al. (2010), Evidence for a flux transfer event generated by multiple X-line reconnection at the magnetopause, *Geophys. Res. Lett.*, *37*, L16101, doi:10.1029/2010GL044219.

Hidalgo, M. A., C. Cid, A. F. Vinas, and J. Sequeiros (2002a), A non-force-free approach to the topology of magnetic clouds in the solar wind, *J. Geophys. Res.*, *107*(A1), 1002, doi:10.1029/2001JA900100.

Hidalgo, M. A., T. Nieves-Chinchilla, and C. Cid (2002b), Elliptical cross-section model for the magnetic topology of magnetic clouds, *Geophys. Res. Lett.*, *29*(13), 1637, doi:10.1029/2001GL013875.

Kobel, E., and E. O. Flückiger (1994), A model of the steady state magnetic field in the magnetosheath, *J. Geophys. Res.*, *99*, 23,617–23,622, doi:10.1029/94JA01778.

Korth, H., B. J. Anderson, J. M. Raines, J. A. Slavin, T. H. Zurbuchen, C. L. Johnson, M. E. Purucker, R. M. Winslow, S. C. Solomon, and R. L. McNutt Jr. (2011), Plasma pressure in Mercury's equatorial magnetosphere derived from MESSENGER Magnetometer observations, *Geophys. Res. Lett.*, *38*, L22201, doi:10.1029/2011GL049451.

Kuznetsova, M. M., and L. M. Zeleny (1986), Spontaneous reconnection at the boundaries of planetary magnetospheres, in *Proceedings of the Joint Varenna-Abastumani International School and Workshop on Plasma Astrophysics*, *Spec. Publ. 251*, pp. 137–146, Eur. Space Agency, Noordwijk, Netherlands.

Lee, L. C., and Z. F. Fu (1985), A theory of magnetic flux transfer at the Earth's magnetopause, *Geophys. Res. Lett.*, *12*, 105–108, doi:10.1029/GL012i002p00105.

Lepping, R. P., J. A. Jones, and L. F. Burlaga (1990), Magnetic field structure of interplanetary magnetic clouds at 1 AU, *J. Geophys. Res.*, *95*, 11,957–11,965, doi:10.1029/JA095iA08p11957.

Liu, J., V. Angelopoulos, D. Sibeck, T. Phan, Z. Y. Pu, J. McFadden, K. H. Glassmeier, and H. U. Auster (2008), THEMIS observations of the dayside traveling compression region and flows surrounding flux transfer events, *Geophys. Res. Lett.*, *35*, L17S07, doi:10.1029/2008GL033673.

Lockwood, M., and M. N. Wild (1993), On the quasi-periodic nature of magnetopause flux transfer events, *J. Geophys. Res.*, *98*, 5935–5940, doi:10.1029/92JA02375.

Moldovan, R., B. J. Anderson, C. L. Johnson, J. A. Slavin, H. Korth, M. E. Purucker, and S. C. Solomon (2011), Mercury's magnetopause and bow shock from MESSENGER observations, Abstract EPSC-DPS2011-674 presented at EPSC-DPS Joint Meeting 2011, Eur. Planet. Sci. Congress, Nantes, France.

Moldwin, M. B., M. R. Collier, J. A. Slavin, and A. Szabo (2001), On the origin of reverse polarity TCRs, *Geophys. Res. Lett.*, *28*, 1925–1928, doi:10.1029/2000GL012485.

Owen, C. J., A. Marchaudon, M. W. Dunlop, A. N. Fazakerley, J.-M. Bosqued, J. P. Dewhurst, R. C. Fear, S. A. Fuselier, A. Balogh, and H. Rèmy (2008), Cluster observations of "crater" flux transfer events in the dayside high-latitude magnetopause, *J. Geophys. Res.*, *113*, A07S04, doi:10.1029/2007JA012701.

Pilipp, W. G., and G. Morfill (1978), The formation of the plasma sheet resulting from plasma mantle dynamics, *J. Geophys. Res.*, *83*, 5670–5678, doi:10.1029/JA083iA12p05670.

Raeder, J. (2006), Flux transfer events: 1. Generation mechanism for strong southward IMF, *Ann. Geophys.*, *24*, 381–392, doi:10.5194/angeo-24-381-2006.

Rijnbeek, R. P., S. W. H. Cowley, D. J. Southwood, and C. T. Russell (1984), A survey of dayside flux transfer events observed by ISEE 1 and 2 magnetometers, *J. Geophys. Res.*, *89*, 786–800, doi:10.1029/JA089iA02p00786.

Russell, C. T., and R. C. Elphic (1978), Initial ISEE magnetometer results: Magnetopause observations, *Space Sci. Rev.*, *22*, 681–715, doi:10.1007/BF00212619.

Russell, C. T., and R. J. Walker (1985), Flux transfer events at Mercury, *J. Geophys. Res.*, *90*, 11,067–11,074, doi:10.1029/JA090iA11p11067.

Slavin, J. A., and R. E. Holzer (1979), The effect of erosion on the solar wind stand-off distance at Mercury, *J. Geophys. Res.*, *84*, 2076–2082, doi:10.1029/JA084iA05p02076.

Slavin, J. A., M. F. Smith, E. L. Mazur, D. N. Baker, E. W. Hones Jr., T. Iyemori, and E. W. Greenstadt (1993), ISEE 3 observations of traveling compression regions in the Earth's magnetotail, *J. Geophys. Res.*, *98*, 15,425–15,446, doi:10.1029/93JA01467.

Slavin, J. A., et al. (2008), Mercury's magnetosphere after MESSENGER's first flyby, *Science*, *321*, 85–89, doi:10.1126/science.1159040.

Slavin, J. A., et al. (2009), MESSENGER observations of magnetic reconnection in Mercury's magnetosphere, *Science*, *324*, 606–610, doi:10.1126/science.1172011.

Slavin, J. A., et al. (2010), MESSENGER observations of large flux transfer events at Mercury, *Geophys. Res. Lett.*, *37*, L02105, doi:10.1029/2009GL041485.

Solomon, S. C., R. L. McNutt Jr., R. E. Gold, and D. L. Domingue (2007), MESSENGER mission overview, *Space Sci. Rev.*, *131*, 3–39, doi:10.1007/s11214-007-9247-6.

Sonnerup, B. U. O. (1974), Magnetopause reconnection rate, *J. Geophys. Res.*, *79*, 1546–1549, doi:10.1029/JA079i010p01546.

Spreiter, J. R., A. L. Summers, and A. Y. Alksne (1966), Hydromagnetic flow around the magnetosphere, *Planet. Space Sci.*, *14*, 223–253, doi:10.1016/0032-0633(66)90124-3.

Trenchi, L., M. F. Marcucci, H. Rème, C. M. Carr, and J. B. Cao (2011), TC-1 observations of a flux rope: Generation by multiple X line reconnection, *J. Geophys. Res.*, *116*, A05202, doi:10.1029/2010JA015986.

Wang, Y. L., et al. (2005), Initial results of high-latitude magnetopause and low-latitude flank flux transfer events from 3 years of Cluster observations, *J. Geophys. Res.*, *110*, A11221, doi:10.1029/2005JA011150.

Zhang, H., K. K. Khurana, M. G. Kivelson, V. Angelopoulos, Z. Y. Pu, Q.-G. Zong, J. Liu, and X.-Z. Zhou (2008), Modeling a force-free flux transfer event probed by multiple THEMIS spacecraft, *J. Geophys. Res.*, *113*, A00C05, doi:10.1029/2008JA013451.

Zong, Q.-G., et al. (2005), Plasmoid in the high latitude boundary/cusp regions observed by Cluster, *Geophys. Res. Lett.*, *32*, L01101, doi:10.1029/2004GL020960.

Zurbuchen, T. H., et al. (2011), MESSENGER observations of the spatial distribution of planetary ions near Mercury, *Science*, *333*, 1862–1865, doi:10.1126/science.1211302.